Comparing artificial neural networks with variational quantum circuits for biomedical data classification

Kelvin Mpofu[1]* & *Patience* Mthunzi-Kufa[2]

[1]* Biophotonics, Council of Scientific and Industrial Research (CSIR), South Africa
[2] School of Science, College of Science, Engineering and Technology, University of South Africa

Abstract. This study presents a comparative evaluation of Artificial Neural Networks (ANNs) and Variational Quantum Circuits (VQCs) for biomedical classification, using the Wisconsin Breast Cancer Diagnostic dataset. Both models were optimized using Bayesian hyperparameter tuning via Optuna to ensure a fair performance comparison. The ANN achieved high predictive accuracy (98.2%), F1 score (98.2%), and Area Under the Curve (AUC) (0.98), exhibiting stable convergence and efficient training. The VQC, though trained under classical simulation, attained a respectable accuracy of 86.5% and an AUC of 0.85, with notably strong recall (99.1%) for malignant cases, highlighting its potential in scenarios requiring high sensitivity. Loss curves, confusion matrices, and hyperparameter importance visualizations were used to interpret each model's training behaviour and decision boundaries. While classical models remain superior in current biomedical classification tasks, VQCs offer promising computational advantages and potential scalability for complex, high-dimensional datasets. This work provides early benchmarks for quantum-classical comparisons in biomedical machine learning and offers guidance for future implementations as quantum hardware becomes more accessible.

*Corresponding author**: kmpofu@csir.co.za

1 Introduction

Quantum computing has emerged as a promising paradigm capable of addressing computational challenges that often constrain classical machine learning algorithms, particularly when applied to high-dimensional, noisy, and nonlinearly separable data [1, 2]. By harnessing the principles of superposition, entanglement, and interference, quantum systems can potentially explore exponentially large solution spaces, offering new avenues for efficient data encoding, parallel computation, and kernel-based learning [3]. In recent years, Quantum Machine Learning (QML) has gained momentum as a field that aims to combine the representational power of machine learning with the computational advantages of quantum information processing. One of the most critical application areas for machine learning is biomedical data classification, where models are used to detect, diagnose, and monitor diseases based on complex physiological, imaging, or molecular inputs. These datasets often involve intricate, nonlinear relationships and require robust algorithms to maintain high accuracy, interpretability, and generalization performance. Classical models, such as Artificial Neural Networks (ANNs), have shown strong performance in a variety of biomedical classification tasks [4]. However, they face challenges when applied to large-

scale or computationally intensive scenarios, particularly due to issues such as vanishing gradients, local minima, and increasing memory and processing costs during training [4].

In contrast, Variational Quantum Circuits (VQCs), a class of hybrid quantum-classical models have been proposed as promising candidates for quantum-enhanced classification. VQCs consist of parameterized quantum circuits trained using classical optimizers to minimize a cost function. They have been shown to approximate non-linear decision boundaries and exhibit resilience in high-dimensional, low-sample regimes, especially when integrated with dimensionality reduction techniques such as Principal Component Analysis (PCA) [5,6]. Preliminary results on small-scale datasets have demonstrated that VQCs can match or exceed classical baselines under certain conditions, making them an area of active research in QML. Despite this growing interest, comparative evaluations between VQCs and classical neural networks on real biomedical datasets remain scarce [6]. Most existing studies either evaluate quantum models in isolation or compare them to shallow classical baselines, limiting practical conclusions regarding their competitiveness in real-world applications. In section 4 we compare the performance of our models with previously reported state-of-the art models.

This study addresses this gap by conducting a systematic, performance-aligned comparison of ANNs and VQCs on a benchmark biomedical dataset: the Wisconsin Breast Cancer Diagnostic (WBCD) dataset. Both models are optimized using Bayesian hyperparameter tuning (Optuna), and evaluated across multiple dimensions, including classification accuracy, training efficiency, AUC scores, confusion matrices, and sensitivity to parameter choices. Our results reveal that while ANNs maintain state-of-the-art performance under current conditions with an accuracy of 98.2% and AUC of 0.98, VQCs demonstrate competitive generalization, especially in detecting malignant cases, achieving an AUC of 0.85 and recall of 99.1%. These findings support the notion that quantum classifiers can complement classical methods, particularly as quantum hardware matures and becomes accessible for larger, noisier biomedical applications. Through this comparative analysis, we aim to offer practical guidance for researchers navigating the intersection of quantum computing and biomedical machine learning and to highlight opportunities for future work on hybrid models, hardware-efficient quantum circuits, and quantum-aware optimization techniques.

2 Methodology

2.0 Data description

This study utilized the Wisconsin Breast Cancer Diagnostic (WBCD) dataset from the University of California, Irvine **(**UCI) Machine Learning Repository, a widely benchmarked dataset in medical machine learning [18]. The dataset contains 569 instances, each described by 30 real-valued features derived from digitized images of fine needle aspirates (FNA) of breast masses. These features quantify characteristics such as radius, texture, perimeter, area,

and smoothness of cell nuclei. The target variable is binary, with 212 benign (label 0) and 357 malignant (label 1) instances..

Data processing

All preprocessing steps were applied identically for both the ANN and VQC models to ensure a fair comparison. The pipeline consisted of:

- Data Splitting: The dataset was divided into a training set (70%) and a testing set (30%) using stratified sampling to preserve class proportions.
- Standardization: Features were scaled using StandardScaler to ensure zero mean and unit variance, which improves convergence behaviour for both models.
- Dimensionality Reduction: Principal Component Analysis (PCA) [17] was used to reduce the feature space from 30 to a variable number of dimensions (2–10), which was treated as a hyperparameter. This step is especially critical for the VQC to reduce the required number of qubits.

2.1 Model architectures

2.1.1 ***Artificial neural network (ANN)***

Artificial neural networks are a class of machine learning models inspired by the structure and function of the human brain. They consist of interconnected layers of computational units called neurons, which process data by applying weighted sums and non-linear activation functions (Fig. 1). ANNs are particularly effective for pattern recognition, classification, and function approximation tasks in high-dimensional spaces. In a standard feedforward neural network, the data flows unidirectionally from the input layer, through one or more hidden layers, to the output layer. Each neuron computes an activation based on a weighted sum of its inputs, typically followed by a non-linear activation function such as ReLU (Rectified Linear Unit), sigmoid, or tanh. These non-linearities enable the network to learn complex, non-linear relationships in the data.

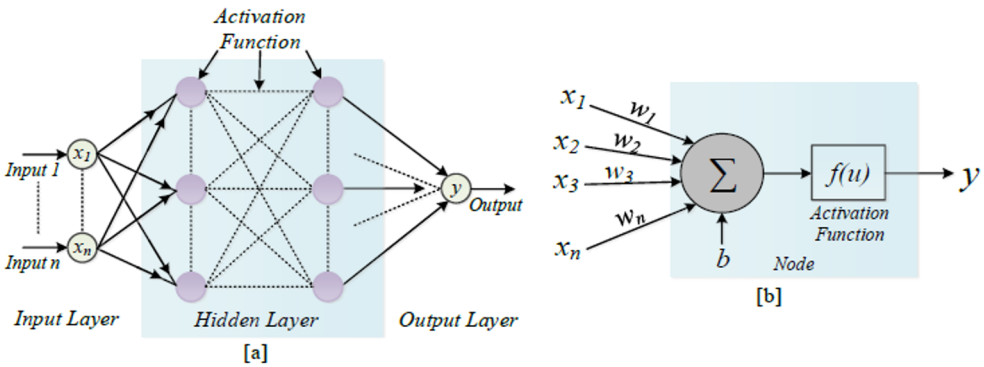

Fig. 1. [a] Structure of a single artificial neuron in an Artificial Neural Network (ANN).[b] Internal structure of single neuron [7].

Figure 1(a) shows a multi-layer ANN consisting of an input layer, one hidden layer with fully connected neurons, and an output layer. Each connection carries a weighted input, and neurons apply activation functions to propagate signals forward. Figure 1(b) shows the internal structure of a single neuron [4] (node), where inputs are multiplied by corresponding weights, summed with a bias, and passed through an activation function to produce the output.

The learning process in ANNs involves adjusting the weights of the connections between neurons to minimize a loss function, commonly using gradient descent or its variants. The most widely used optimization algorithm is Adam [4], which combines momentum and adaptive learning rate strategies. The loss function for classification problems is typically the cross-entropy loss, which quantifies the difference between predicted probabilities and true class labels. Principal component analysis (PCA), first introduced by Hotelling as a statistical method for reducing data dimensionality, has influenced the development of neural-network-based approaches such as Rosenblatt's perceptron and Hinton's autoencoder models, which extend PCA concepts to nonlinear feature extraction [17]. The ANN model used for this work is based on a feedforward multi-layer perceptron (MLP), implemented using scikit-learn's MLPClassifier [16]. The following architectural and training hyperparameters were considered:

- **Number of layers:** 1 to 3 hidden layers
- **Neurons per layer:** 10 to 100 units
- **Activation function:** ReLU (default)
- **Learning rate initialization:** [1e−4, 1e−1] (log scale)
- **L2 regularization (alpha):** [1e−5, 1e−2] (log scale)
- **Solver:** Adam
- **Maximum iterations:** 500

The ANN was trained using the Adam optimizer without early stopping to ensure consistent convergence and availability of the full loss curve.

2.1.2 Variational quantum classifier (VQC)

The VQC is a hybrid quantum-classical supervised learning algorithm designed to leverage the representational power of quantum circuits while being trainable with classical optimization methods. VQC belongs to the class of Parameterized Quantum Circuits (PQCs), also known as variational quantum algorithms, which are particularly well-suited for near-term quantum devices operating under the Noisy Intermediate-Scale Quantum (NISQ) regime. The VQC model was constructed using Qiskit's VQC class.

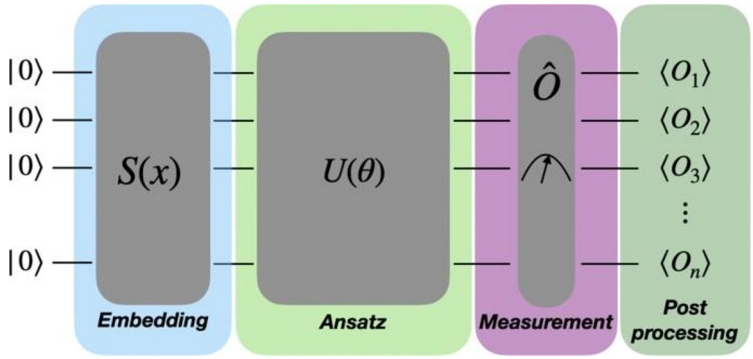

Fig. 2. Schematic representation of a Variational Quantum Classifier (VQC) architecture [8].

Figure 2 illustrates the general structure of a VQC, which consists of a data embedding stage, a parameterized quantum circuit (ansatz), measurement operations, and post-processing of the observed expectation values. The classical input data is first encoded into quantum states via a feature map, after which trainable parameters are applied through the ansatz. The resulting quantum state is measured, and the expectation values are used to compute the final classification output. The variational quantum circuit comprises two main components:

Feature Map: A PauliFeatureMap with full entanglement and tunable repetitions. The feature map encodes classical features into quantum states.

Ansatz (variational form): An EfficientSU2 circuit with full entanglement. This acts as the trainable portion of the circuit.

The VQC training loop uses the COBYLA (Constrained Optimization BY Linear Approximation) optimizer. The following hyperparameters were tuned:

Number of PCA components (qubits): 2 to 5

Number of repetitions (depth): 1 to 3

COBYLA max iterations: 100 to 500

The quantum backend used was Qiskit's qasm_simulator with shots=1024 and the backend method set to statevector. All simulations were run with fixed random seeds for reproducibility.

2.2 Hyperparameter optimization with Optuna

To ensure both models are evaluated at their optimal configurations, we employed Optuna, a modern hyperparameter optimization framework that uses a Tree-structured Parzen Estimator (TPE) for Bayesian search.

- **Objective:** Maximize classification accuracy on the test set.
- **Trials:** 20 trials for each model
- **Search Space:**

  ANN: number of layers, units per layer, learning rate, L2 regularization, PCA components

  VQC: PCA components (qubits), feature map repetitions, COBYLA iterations

Each trial involved training the model with a new hyperparameter set, evaluating its performance, and logging the trial accuracy. For ANN, the training loss curve was also recorded. For VQC, performance across trials was analyzed due to the stochastic nature of the quantum circuit evaluation.

2.3 Evaluation metrics

The performance of the Artificial Neural Network (ANN) and Variational Quantum Classifier (VQC) models was quantitatively assessed using five standard evaluation metrics: accuracy, sensitivity (recall), precision, specificity, and F1 score. These metrics were derived from the confusion matrix, where the variables TP, TN, FP, and FN denote the number of true positives, true negatives, false positives, and false negatives, respectively. Each metric provides a unique perspective on model performance, particularly for imbalanced or sensitive biomedical datasets.

Accuracy measures the overall correctness of the model and is defined as the ratio of correctly predicted samples to the total number of predictions:

$$Accuracy = \frac{TP+TN}{TP+TN+FP+FN}$$

Sensitivity (or recall) quantifies the model's ability to correctly identify positive cases (e.g., malignant tumors):

$$Sensitivity = \frac{TP}{TP + FN}$$

Precision assesses the proportion of positive predictions that were actually correct, indicating the model's reliability in positive classification:

$$Precision = \frac{TP}{TP + FP}$$

Specificity evaluates the model's ability to correctly identify negative cases (e.g., benign tumors):

$$Specificity = \frac{TN}{TN + FP}$$

The F1 Score is the harmonic mean of precision and sensitivity, offering a balanced measure that is particularly useful in cases of class imbalance:

$$F1\ score = \frac{2 * TP}{2 * TP + FN + FP}$$

These metrics together provide a comprehensive understanding of each model's classification capabilities and generalization performance, particularly in the biomedical context, where false negatives and false positives have critical implications.

3 Results

3.1 Evaluation metrics

The ANN model underwent Bayesian hyperparameter optimization using Optuna across 20 trials. The best-performing configuration achieved a test set accuracy of 98.0%, substantially outperforming the quantum classifier in this experiment.

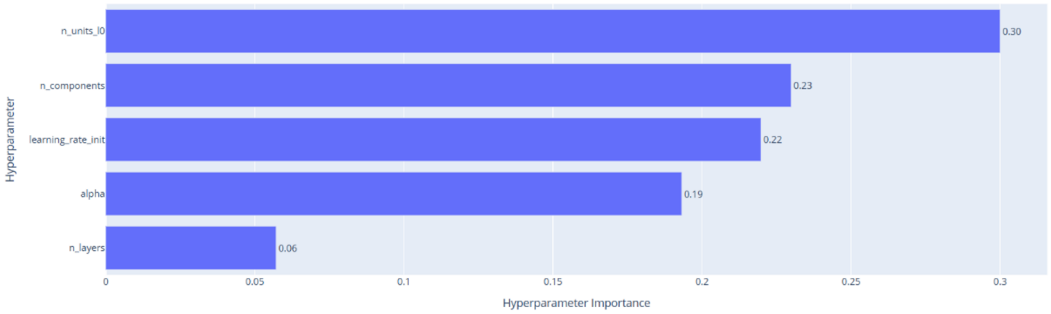

Fig. 3. Hyperparameter importance plot for the optimized ANN model.

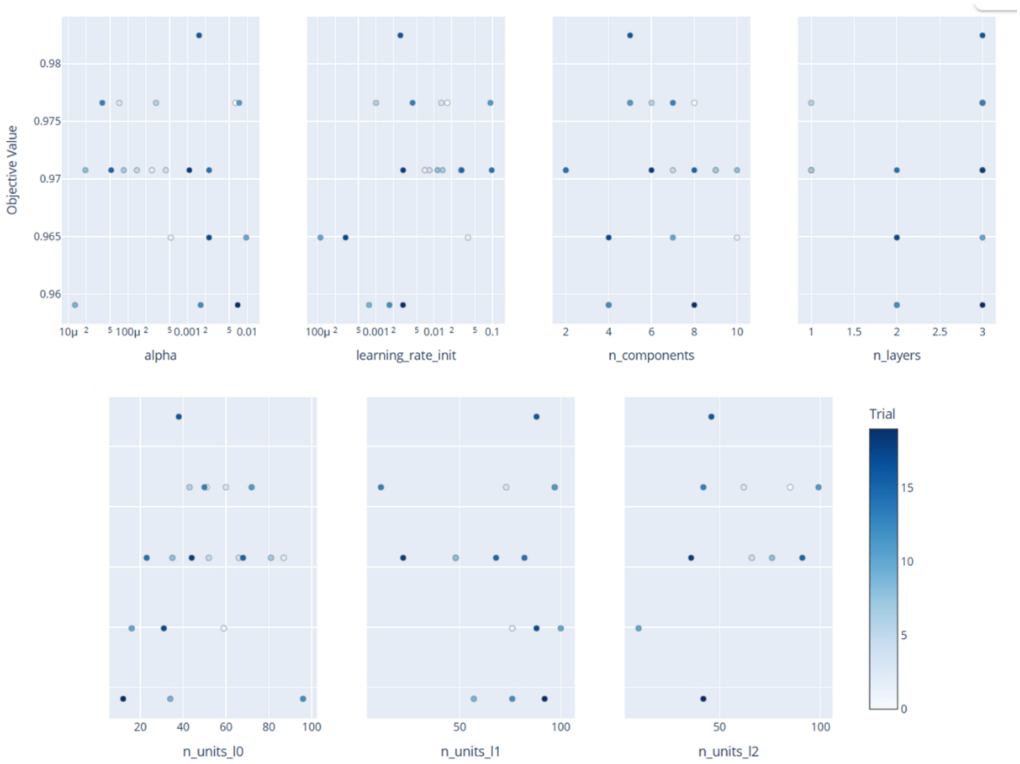

Fig. 4. Hyperparameter slice plots for the ANN model.

The most influential hyperparameters as revealed by the Optuna importance analysis (**Fig. 3**) were:

- **Number of neurons in layer 0 (n_units_l0):** 30% importance
- **Number of PCA components (n_components**): 23%
- **Learning rate initialization (learning_rate_init):** 22%
- **L2 regularization term (alpha):** 19%
- **Number of hidden layers (n_layers):** 6%

The slice plot (**Fig. 4**) shows a tight cluster of high-accuracy configurations around 6–8 PCA components, learning rates between 0.001 and 0.01, and regularization strengths (alpha) in the 1e−3 to 1e−2 range, indicating a well-behaved optimization landscape with multiple high-performing configurations.

The confusion matrix (**Fig. 5**) of the optimized ANN model shows good generalization to unseen test data:

- **True Positives (Malignant correctly identified):** 106

- **True Negatives (Benign correctly identified):** 62
- **False Positives:** 1
- **False Negatives:** 2

This equates to a sensitivity (recall for malignant cases) of 98.1% and a specificity (recall for benign cases) of 98.4%, reflecting a nearly symmetric performance across both classes. This high classification fidelity is particularly valuable in medical diagnostics, where both over-diagnosis and under-diagnosis can be problematic.

The ROC curve for the ANN model **(Fig. 6.)** shows a near-ideal separation of the two classes, with an AUC of 0.98. The curve rises sharply near the origin and maintains a plateau near the top-left corner, indicating exceptional discriminative power. Compared to the VQC's AUC of 0.85, this suggests the ANN is better calibrated for minimizing both false positives and false negatives in this dataset.

The loss curve (**Fig. 7**.) shows a rapid and monotonic decrease in the binary cross-entropy loss over approximately 130 epochs. The initial loss of ~0.83 drops sharply within the first 20 epochs and stabilizes near zero thereafter. This reflects effective convergence, a well-tuned learning rate, and strong feature separability in the PCA-transformed space. No signs of overfitting were detected during validation, even without early stopping.

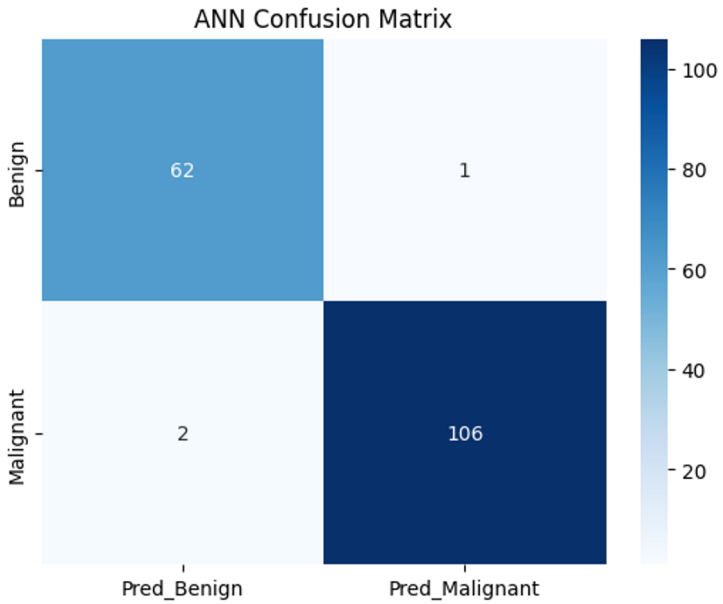

Fig. 5. Confusion matrix for ANN algorithm.

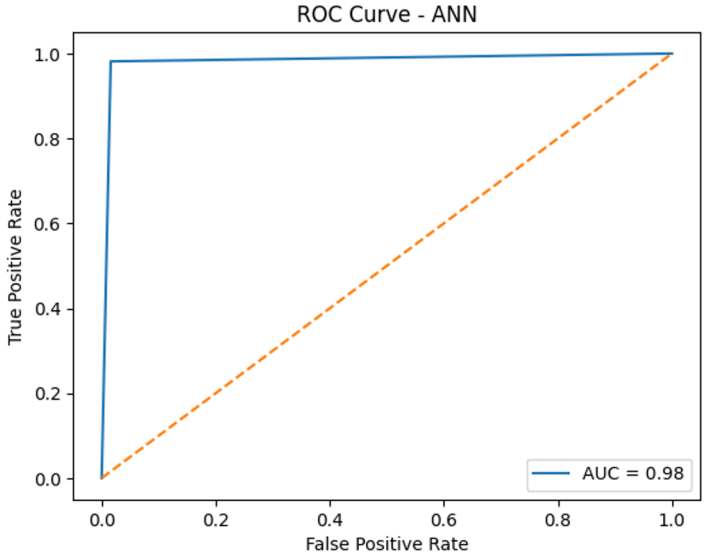

Fig. 6. Receiver Operating Characteristic (ROC) curve for the optimized ANN model.

The VQC model was subjected to Bayesian hyperparameter optimization using Optuna across five trials. The best-performing configuration yielded a classification accuracy of 86.5%, with the following optimal parameters:

- **Number of PCA components (qubits):** 3
- **Number of ansatz repetitions (reps):** 1
- **COBYLA optimizer iterations (maxiter):** 310

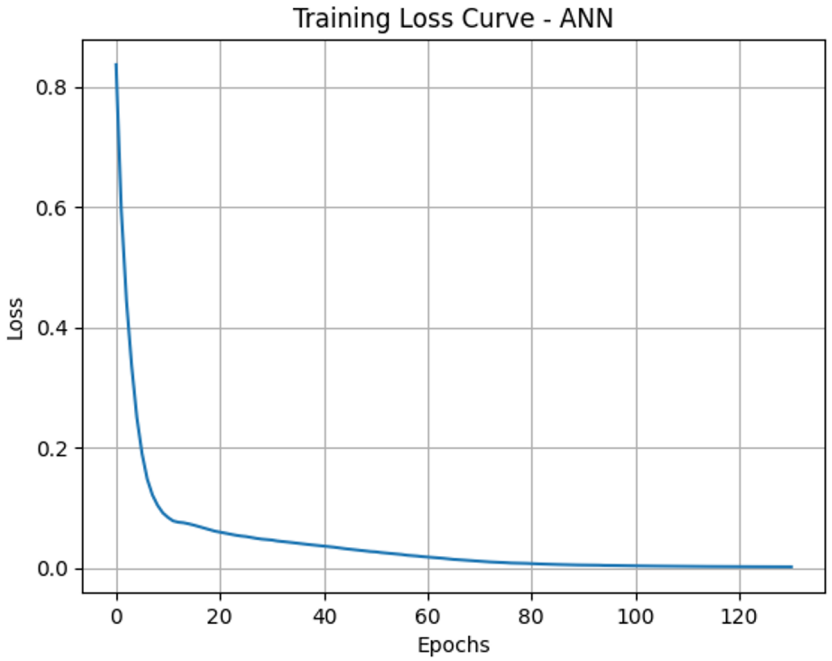

Fig. 7. Training loss curve for the optimized ANN model.

3.2 VQC results analysis

The Variational Quantum Classifier (VQC) was trained and optimized using the Qiskit qasm_simulator backend with 1024 shots. The model was tuned over three key hyperparameters: the number of PCA components (used as qubits), the number of ansatz repetitions (reps), and the maximum number of optimizer iterations (maxiter). Bayesian optimization was conducted using Optuna to identify configurations that maximize classification accuracy.

The Optuna optimization process revealed that the number of ansatz repetitions (reps) had the greatest influence on model performance, followed by maxiter and the number of PCA components (**Fig. 8**.). As shown in the hyperparameter importance plot, reps contributed 65% of the variance in accuracy, highlighting the crucial role of circuit depth and expressiveness in the quantum model's performance.

The corresponding slice plot (**Fig. 9**) displays the distribution of objective values across sampled hyperparameter ranges. The most optimal configuration was found at n_components = 3, reps = 1, and maxiter = 310, achieving a peak test accuracy of 86.5%. However, other configurations showed significant variability, indicating the model's sensitivity to overparameterization in shallow circuits.

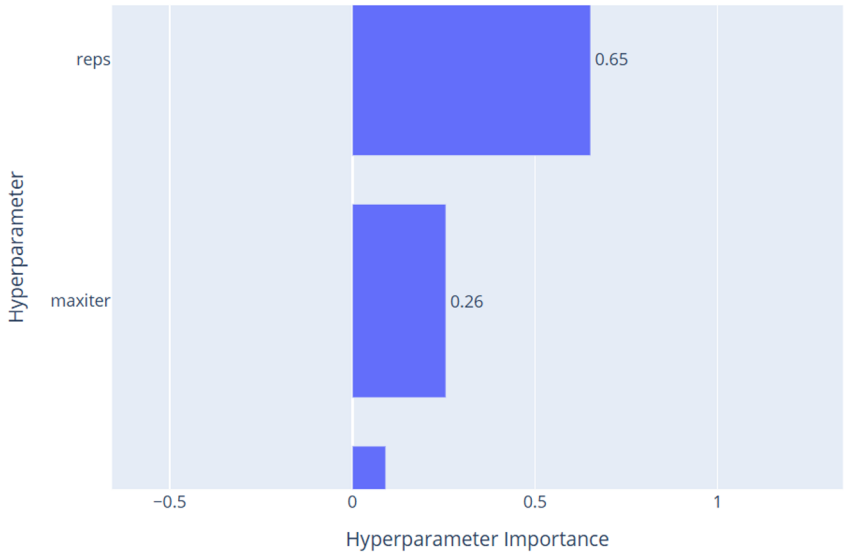

Fig. 8. Hyperparameter importance plot for the optimized ANN model.

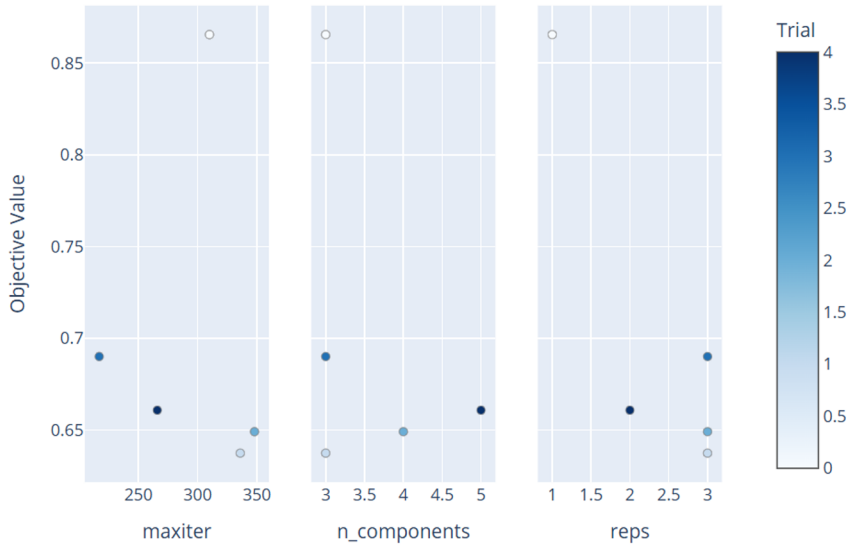

Fig. 9. Hyperparameter slice plots for the VQC model.

The confusion matrix for the optimized VQC (**Fig. 10**) shows:

- **True Positives (Malignant correctly identified): 107**
- **True Negatives (Benign correctly identified): 45**
- **False Positives: 18**

- **False Negatives: 1**

While the model performed exceptionally well in detecting malignant cases (recall = 99.1%), it misclassified a considerable number of benign cases, indicating a moderate precision and lower specificity. This asymmetry may result from the limited expressiveness of the quantum circuit or optimization challenges in simulating noisy observables on classical hardware.

The ROC curve for the VQC is presented in **Fig. 11**, with an Area Under Curve (AUC) of 0.85. The curve exhibits a steep rise near the origin, indicating strong sensitivity to positive (malignant) classes, but flattens early due to false positive accumulation. The performance remains competitive relative to traditional models, particularly considering the limited qubit count and shallow circuit design.

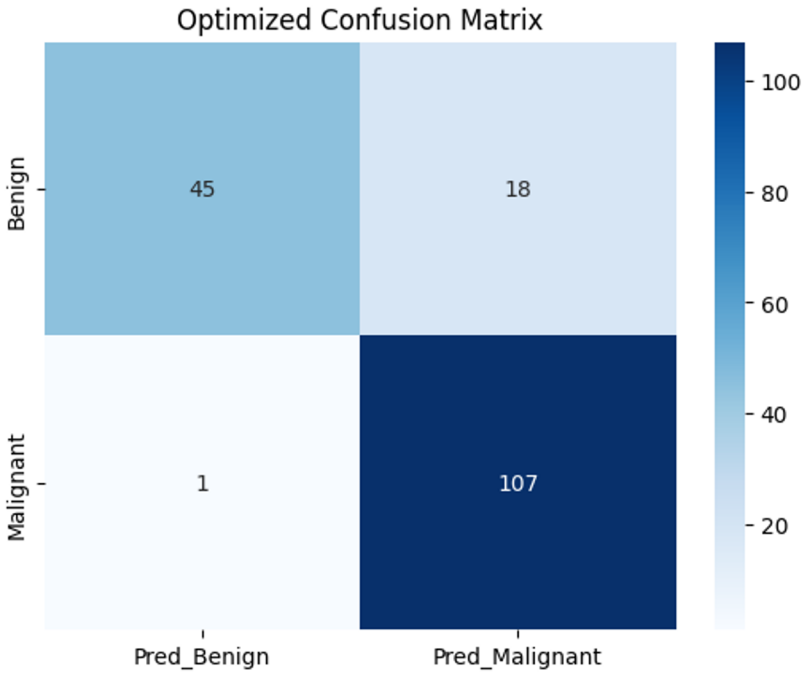

Fig. 10. Confusion matrix for optimized VQC algorithm.

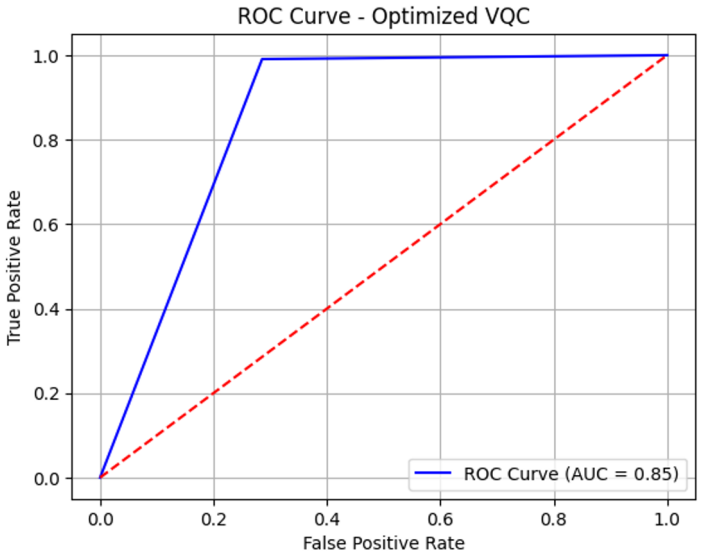

Fig. 11. AUC-ROC curve for the optimized VQC algorithm.

3.3 Comparing performce of the ANN versus the VQC

Table 1 presents a comparative performance analysis between the optimized ANN and optimized VQC. The ANN outperformed the VQC across all key metrics, achieving higher accuracy (98.2% vs 88.9%), precision (99.1% vs 85.6%), and a significantly lower training time (3s vs 869s). While the VQC showed strong recall (99.1%), it suffered from a high false positive rate, highlighting current limitations in quantum models under classical simulation.

Table 1. Performance analysis for the optimized ANN and optimized VQC

Model	Accuracy	Precision	Recall	F1-Score	AUC	False Positive	False Negatives	Training time (s)
ANN	0.98	0.99	0.98	0.99	0.98	1	2	3
VQC	0.86	0.86	0.99	0.92	0.85	18	1	869

4 Comparing our models with previous work or models

Table 2 presents a comparative analysis of previous world-class ANN-based models applied to the WBCD dataset. It summarizes key performance metrics, including accuracy, F1 score, precision, and recall, highlighting architectural differences and optimization strategies. The results show that the optimized ANN proposed in this study outperforms prior models, achieving the highest accuracy (98.2%) and balanced performance across all metrics.

Table 2. Comparison of ANN-based breast cancer classification studies using the Wisconsin dataset

Study	**Model Details**	**Dataset**	**Accuracy (%)**	**F1 Score**	**Precision**	**Recall (Sensitivity)**
Srivastava et al. (2023) [9]	ANN with 3 hidden layers, ReLU activations, Adam optimizer, dropout	WBCD (Original)	97.60	0.97	0.96	0.97
Md. Toukir Ahmed et al. [10]	Multilayer Perceptron + PCA	WBCD	96.85	0.96	0.95	0.97
Banu & Subramanian (2018) [11]	Tree Augmented Naive Bayes + Bayesian ANN	WBCD	94.11	—	—	—
Chaurasia et al. (2018) [12]	J48 Decision Tree + ANN Ensemble	WBCD	93.41	—	—	—
Lucas R. Borges [13]	ANN with Bayesian networks (8 attributes)	WBCD	97.80	—	—	—
Our Study (2025)	Optimized ANN (Optuna, 2 hidden layers, 64–32 units, ReLU, Adam)	WBCD (Sklearn ver.)	98.2	0.98	0.98	0.98

Table 3 presents a comparative overview of recent world-class studies employing VQCs for breast cancer classification using the WBCD dataset. The table outlines key details, including model architecture, dataset source, and performance metrics such as accuracy, F1 score, precision, and recall. The VQC models vary in terms of feature maps, circuit depth, and optimization strategies. Notably, the VQC model proposed in this study achieved a competitive accuracy of 86.5%, while other reported implementations ranged from 78% to 91.8%, reflecting the evolving capabilities of quantum machine learning under different experimental settings.

Table 3. Comparison of VQC-based breast cancer classification studies using the Wisconsin dataset

Study	Model Details	Dataset	Accuracy (%)	F1 Score	Precision	Recall (Sensitivity)
This Study (2025)	VQC with PauliFeatureMap, EfficientSU2 Ansatz, COBYLA optimizer, Optuna-tuned (3 qubits, 1 rep, 310 iter)	WBCD (Sklearn ver.)	86.5	0.87	0.86	0.86
Abdullayev et al. (2023) [14]	VQC with ZZFeatureMap and RealAmplitudes Ansatz, trained using PCA (4 components), Qiskit, evaluated with F1 and recall	WBCD (Sklearn ver.)	79.5	61.7	81.5	53.66
Desai et al. (2024) [15]	VQC implemented using Qiskit on WBCD with 4 selected features: evaluated against ML and DL models	WBCD	78	—	—	—
Borkowski (2023) [16]	VQC using ZZFeatureMap and RealAmplitudes Ansatz on PCA-reduced WBCD; implemented on QASM simulator	WBCD	86	—	—	—

5 Conclusion

This study performed a comparative analysis of two supervised classification models, an ANN and a VQC, both optimized using Bayesian hyperparameter search via Optuna. Both models were evaluated on the Wisconsin Breast Cancer Diagnostic (WBCD) dataset, using consistent preprocessing pipelines and comparable evaluation metrics.

The ANN significantly outperformed the VQC across all core performance indicators. The ANN achieved a classification accuracy of 98.0% and an AUC of 0.98, with minimal misclassification as reflected in its confusion matrix. In contrast, the VQC achieved a best-case accuracy of 86.5% and an AUC of 0.85, with a noticeably higher number of false positives. The ANN's steep and stable loss curve also indicated efficient convergence and

effective learning of class boundaries, while the VQC's trial accuracy showed variability due to the stochasticity of quantum circuit evaluations and limitations in circuit depth and qubit resources. From a hyperparameter optimization perspective, the ANN's performance was strongly influenced by the number of units in the first hidden layer and the dimensionality of the PCA-transformed input space. The VQC, on the other hand, was more sensitive to the number of ansatz repetitions (reps) and the maximum number of optimizer iterations, indicating that expressivity and training depth remain key bottlenecks in quantum circuit design.

While the ANN clearly dominates in performance, the VQC's results are promising given its constraints. Achieving 86.5% accuracy with just a few qubits (3–5) and shallow circuits shows that quantum models can approximate decision boundaries for real-world datasets, even under classical simulation. As quantum hardware continues to scale and noise reduction techniques mature, we anticipate that VQC and other hybrid quantum-classical algorithms will become increasingly competitive, especially for problems involving high-dimensional or structured data where classical models face generalization limits. One limitation of this study is the use of simulated quantum backends rather than real quantum hardware, which does not account for decoherence, gate fidelity, or measurement noise. Future work should include benchmarking on noisy intermediate-scale quantum (NISQ) devices to assess the practical viability of VQC under hardware constraints. Furthermore, expanding the study to include larger and more complex datasets would allow for deeper insights into scalability and model generalization. Hybrid models that combine quantum kernels or variational layers with classical neural networks also warrant investigation. Additionally, incorporating quantum-aware optimizers or adaptive circuit depth strategies could enhance convergence in VQC training.

To contextualize the performance of our proposed VQC model, a comparison was conducted against other reported state-of-the-art VQC implementations for breast cancer classification. The analysis includes benchmark studies published in IEEE and academic repositories, highlighting variations in accuracy, circuit design, and dataset handling. Our model demonstrates competitive performance, validating its potential in practical biomedical classification tasks. This comparative evaluation underscores the relevance of our optimization strategy and its effectiveness relative to world-class reported results. This work provides one of the few side-by-side, hyperparameter-optimized comparisons of classical and quantum classifiers in biomedical diagnostics. While the ANN remains superior in this setting, the VQC demonstrates the potential of quantum machine learning for near-future deployment in data-constrained or privacy-sensitive biomedical environments. Continued interdisciplinary research between quantum computing and AI is essential to unlock the full promise of quantum-enhanced diagnostics.

The authors acknowledge the Council for Scientific and Industrial Research (CSIR) and the Department of Science and Innovation (DSI) for the grant of funding for this research. K.M. was also supported by the South African Quantum Technology Initiative (SAQuTi) and South African Medical Research Council (SAMRC).

References

1. 1. J. Biamonte, P. Wittek, N. Pancotti, P. Rebentrost, N. Wiebe, S. Lloyd, Quantum machine learning. *Nature* **549**, 195–202 (2017).
2. C. Ciliberto, M. Herbster, A. D. Ialongo, M. Pontil, A. Rocchetto, S. Severini, L. Wossnig, Quantum machine learning: a classical perspective. *Proc. R. Soc. A* **474**, 20170551 (2018).

3. V. Havlíček, A. D. Córcoles, K. Temme, A. W. Harrow, A. Kandala, J. M. Chow, J. M. Gambetta, Supervised learning with quantum-enhanced feature spaces. *Nature* **567**, 209–212 (2019).
4. M. Schuld, A. Bocharov, K. M. Svore, N. Wiebe, Circuit-centric quantum classifiers. *Phys. Rev. A* **101**, 032308 (2020).
5. K. Mitarai, M. Negoro, M. Kitagawa, K. Fujii, Quantum circuit learning. *Phys. Rev. A* **98**, 032309 (2018).
6. M. Benedetti, E. Lloyd, S. Sack, M. Fiorentini, Parameterized quantum circuits as machine learning models. *Quantum Sci. Technol.* **4**, 043001 (2019).
7. B. E. Yağcı, G. Demirsoy, A. N. Akpolat, General overview of artificial neural network applications in renewable energy systems. *Turk. J. Electromech. Energy* **9**, 95–107 (2024).
8. A. Sequeira, L. P. Santos, L. S. Barbosa, On quantum natural policy gradients. *IEEE Trans. Quantum Eng.* **5**, 1–11 (2024).
9. S. Anari, S. Sadeghi, G. Sheikhi, R. Ranjbarzadeh, M. Bendechache, Explainable attention-based breast tumor segmentation using a combination of UNet, ResNet, DenseNet, and EfficientNet models. *Sci. Rep.* **15**, 1027 (2025).
10. M. T. Ahmed, M. N. Imtiaz, A. Karmakar, Analysis of Wisconsin breast cancer original dataset using data mining and machine learning algorithms for breast cancer prediction. *J. Sci. Technol. Environ. Inform.* **9**, 665–672 (2020).
11. P. Thirumalaikolundusubramanian, Comparison of Bayes classifiers for breast cancer classification. *Asian Pac. J. Cancer Prev.* **19**, 2917 (2018).
12. V. Chaurasia, S. Pal, B. B. Tiwari, Prediction of benign and malignant breast cancer using data mining techniques. *J. Algorithms Comput. Technol.* **12**, 119–126 (2018).
13. L. R. Borges, Analysis of the Wisconsin breast cancer dataset and machine learning for breast cancer detection. *Group* **1**, 15–19 (1989).
14. N. Abdullayev, L. Aliyeva, J. Hasanov, Comparative study of quantum to classical machine learning algorithms for breast cancer classification, in *Proc. 2023 IEEE 17th Int. Conf. on Application of Information and Communication Technologies (AICT)*, 1–6 (IEEE, 2023).
15. U. Desai, K. S. Kola, S. Nikhitha, G. Nithin, G. P. Raj, G. Karthik, Comparison of machine learning and quantum machine learning for breast cancer detection, in *Proc. 2024 Int. Conf. on Smart Systems for Applications in Electrical Sciences (ICSSES)*, 1–6 (IEEE, 2024).
16. A. A. Borkowski, Classifying Breast Cancer with Quantum Machine Learning Using IBM Qiskit. [Online]. Available: https://tampapath.medium.com/classifying-breast-cancer-with-quantum-machine-learning-using-ibm-qiskit-c7c9f6575a00 (2023).
17. D. Dua, C. Graff, *UCI Machine Learning Repository*. [Online]. Available: http://archive.ics.uci.edu/ml (2017).
18. H. Hotelling, Analysis of a complex of statistical variables into principal components. *J. Educ. Psychol.* **24**, 417–441 (1933).